COLD MOLECULE PHYSICS

Building one molecule from a reservoir of two atoms

L. R. Liu,[1,2,3] J. D. Hood,[1,3] Y. Yu,[1,2,3] J. T. Zhang,[1,2,3] N. R. Hutzler,[1,2,3]* T. Rosenband,[2] K.-K. Ni[1,2,3]†

Chemical reactions typically proceed via stochastic encounters between reactants. Going beyond this paradigm, we combined exactly two atoms in a single, controlled reaction. The experimental apparatus traps two individual laser-cooled atoms [one sodium (Na) and one cesium (Cs)] in separate optical tweezers and then merges them into one optical dipole trap. Subsequently, photoassociation forms an excited-state NaCs molecule. The discovery of previously unseen resonances near the molecular dissociation threshold and measurement of collision rates are enabled by the tightly trapped ultracold sample of atoms. As laser-cooling and trapping capabilities are extended to more elements, the technique will enable the study of more diverse, and eventually more complex, molecules in an isolated environment, as well as synthesis of designer molecules for qubits.

Chemical reactions proceed through individual collisions between atoms or molecules. However, when performed in stochastic ensembles, the individual reaction probabilities are observed as averages. Crossed molecular beams reduce the thermal velocity dispersion to probe elementary reaction processes based on single collision events, illuminating many aspects of reaction dynamics (*1*–*4*). In quantum degenerate gases, cooled to temperatures <1 μK, the quantum motional degrees of freedom play a critical role in the reaction (*5*–*7*). Comparisons of such experimental reaction rates with theoretical models currently underpin our understanding of reactions at the most elementary level (*8*–*10*).

To further improve the specificity and precision of reaction steps (*11*–*13*), individual particle control is needed, similar to pioneering atom-positioning experiments with scanning tunneling microscopes (*14*), but untethered from surfaces. By controlling individual particles via laser cooling and optical trapping, molecules may be constructed atom by atom while maintaining specific internal and external quantum states.

We realized chemistry in the minimum number regime, where precisely two atoms are brought together to form one molecule with the aid of a photon. We achieved this using movable optical tweezers, in which individual atoms of different elements [in this work, sodium (Na) and cesium (Cs)] are isolated, cooled, manipulated, and eventually combined into a single optical tweezer. With exactly two atoms in an optical tweezer, we can observe their collisions. We can also perform single-molecule spectroscopy in the gas phase by optically exciting the atom pair on a molecular transition, realizing the chemical reaction Na + Cs → NaCs*. Subsequent imaging of Na and Cs fluorescence distinguishes between four possible experimental outcomes: Both, only one, or no atoms are detected in the tweezer, the latter indicating that a reaction has occurred. We chose NaCs for the demonstration because it possesses a large molecular fixed-frame dipole moment of 4.6 D (*15*), making it a strong candidate for a molecular qubit in a future quantum computing architecture.

We began by preparing laser-cooled Na and Cs atoms at a few hundred microkelvin in overlapped magneto-optical traps (MOTs) in a vacuum chamber (10^{-8} Pa). The MOTs serve as cold atom reservoirs for loading single atoms into tightly focused optical tweezer traps (*16*). After loading, the MOTs are extinguished. A schematic of the apparatus is shown in Fig. 1A. The numerical aperture = 0.55 microscope objective focuses two different wavelengths of light, 700 and 976 nm, to waists of 0.7 and 0.8 μm radius. Because of the difference in Na and Cs polarizabilities, the 700-nm-wavelength light attracts Na and repels Cs, whereas 976-nm-wavelength light attracts Cs five times more strongly than does Na (*17*), enabling us to manipulate Na and Cs independently (Fig. 2A). A typical trap depth of 1 mK is achieved for 5 mW of tweezer power.

When tightly confined identical atoms are illuminated with near-atomic-resonant light, light-assisted pairwise collisions result in either zero or one final atom in the trap (*16*, *18*). Single-atom loading succeeds approximately half of the time (*19*). However, the large light shifts for Na in a 700-nm-wavelength tweezer would normally prevent atom cooling and, consequently, efficient atom loading. We eliminated this light shift for Na by alternating the tweezer and cooling beams at a rate of 3 MHz (*20*). Subsequently, Na followed by Cs were imaged, and the polarization gradient was cooled to 70 and 10 μK, respectively. To determine whether an atom is in the optical tweezer, the fluorescence photoelectron counts from each atom in a region of interest (Fig. 1B) are compared with a threshold (Fig. 1C). The fluorescence histograms indicate that the cases of zero or one atom can be distinguished with a fidelity better than 99.97%. We found that in 33% of cases, we loaded a single Na and a single Cs atom side by side. In 18% of cases, no atoms were loaded, and the rest of the time, either a single Na or Cs atom was loaded (Fig. 1B). The experiment, which repeats at 3 Hz, records initial and final fluorescence images in order to determine survival probabilities for different stages of the molecule-formation process.

Once single atoms have been loaded in separate traps, they need to be transported to the same location for molecule formation. Optical tweezers have been used to move single atoms while maintaining atomic internal state coherence (*21*) and to merge two indistinguishable atoms through coherent tunneling into one tweezer (*22*). We adiabatically transported and merged two different atoms, Na and Cs, into the same tweezer by using optical tweezers at two different wavelengths (Fig. 2A). The trap depths were adjusted by changing the beam intensities, and the positions were steered by applying different radio frequencies to the respective acousto-optic deflectors (AODs) (Fig. 1A).

For the merge sequence, the 700-nm tweezer containing Na was kept stationary, while the 976 nm tweezer containing Cs was moved to overlap the atoms (Fig. 2A, I to III). After the merge, the 700-nm tweezer was extinguished adiabatically so as to leave both atoms in the 976-nm tweezer (Fig. 2A, IV). We designed this merge trajectory so that (i) Cs is deeply confined at all times and (ii) the double-well potential imposed on Na is sufficiently asymmetric to avoid a near-degenerate ground state. This process is time-reversible, which enables us to image the atoms separately and determine survival probability.

Because the 700-nm tweezer is extinguished for 1 ms after the merge, while the 976-nm tweezer is always active, the Na atom escapes, unless the two tweezers are overlapped at the end of the merge sequence, whereas the Cs atom is always trapped. The result obtained when scanning the endpoint of the 976-nm tweezer trajectory is shown in Fig. 2B. The height of the Na survival peak at 0 μm of 94(1)% is near the reimaging survival probability of 96% (numbers in parentheses indicate the Wilson score interval).

Having demonstrated adiabatic transport and merging of two species into a tight tweezer, we turned to their collisions. Isolated collisions between two atoms do not usually result in molecule formation because of the need to simultaneously conserve momentum and energy. However, the atoms can change their hyperfine states after colliding, and the exothermic hyperfine-spin-changing collisions impart enough kinetic energy (≈100 mK) to the atoms to eject them from the tweezer (≈1 mK depth) (*23*).

[1]Department of Chemistry and Chemical Biology, Harvard University, Cambridge, MA 02138, USA. [2]Department of Physics, Harvard University, Cambridge, MA 02138, USA. [3]Harvard-MIT Center for Ultracold Atoms, Cambridge, MA 02138, USA.
*Present address: Division of Physics, Mathematics, and Astronomy, California Institute of Technology, Pasadena, CA 91125, USA
†Corresponding author. Email: ni@chemistry.harvard.edu

Generally, a given initial trap occupancy can evolve into four possible outcomes after an experiment: (i) both atoms, (ii) no atoms, (iii) only Cs, and (iv) only Na remain in the trap. Single-atom images from each repetition allow us to post-select on any of these cases and separate one- and two-body processes, giving both lifetimes from a single data set (Fig. 3). For example, when Na and Cs are both present (effective pair density of $n_2 = 2 \times 10^{12}$ cm^{-3}) (*24*), and prepared in a mixture of hyperfine spin states, they are both rapidly lost: $\tau_{loss} = 8(1)$ ms, where τ_{loss} is the $1/e$ time of exponential decay. This yields a loss rate constant $\beta = 5 \times 10^{-11}$ cm^3/s. By contrast, if the atoms are both optically pumped into the lowest-energy hyperfine levels, conservation of energy prevents the change of hyperfine states, and the atom lifetime increases to 0.63(1) s, which is similar to the rate of hyperfine-state relaxation for Cs owing to off-resonant scattering of the tweezer light (*25*). When only one atom is present, one-body loss due to collisions with background gas limits the lifetime to 5 s.

Because of the rapid two-body loss for mixed hyperfine states, we optically pumped each atom into its lowest-energy hyperfine state in order to maintain a long-lived sample of cotrapped Na and Cs atoms. We then performed photoassociation (PA) of the atoms in order to form an excited state molecule, realizing a single instance of the chemical reaction Na + Cs → NaCs*. When illuminating the atoms with resonant PA light, an electronically excited state molecule may form (Fig. 4A) and then rapidly decay to the ground state. The molecule does not scatter imaging light, causing molecule formation to manifest as simultaneous loss of both Na and Cs atoms. These loss resonances are shown in Fig. 4B, bottom, as the frequency of the PA light is scanned below the dissociation threshold.

Our optical tweezer architecture offers a number of advantages for PA measurements over previous methods with bulk samples (*26*). The ability to precisely define the initial reagents eliminates contributions from other reaction processes such as Cs_2 formation or three-body loss. The combination of the high effective pair density $n_2 = 3 \times 10^{12}$ cm^{-3} (*24*), afforded by the tweezer confinement, and high-PA light intensity of 3 kW/cm^2 yields fast PA rates. The high-contrast measurements of single-atom loss result in near-unity molecule detection efficiency and avoid the need for ionization detection (*26*).

We scanned the 200-MHz frequency–broadened PA light from 30 to 250 GHz below the Cs atomic D2 line ($6S_{1/2} - 6P_{3/2}$). We took steps of 200 MHz with 100-ms pulse duration and took an average of approximately 100 repetitions at each data point. An absolute accuracy of 1 GHz was set by the wavemeter. During PA, the Cs atom could be promoted into the upper hyperfine level because of off-resonant scattering of the PA beam, which would lead to spin-changing collisional loss. We counteracted this effect by simultaneously optically pumping Cs into the lower hyperfine level with a separate beam.

The ability to detect molecule formation via atom loss with high efficiency allowed us to probe NaCs* vibrational levels near the dissociation threshold, including resonances that have not been previously observed (Fig. 4). According to ab initio calculations of NaCs* with spin-orbit coupling (*27*), five molecular potentials converge to the Cs ($6P_{3/2}$) + Na ($3S_{1/2}$) asymptote (Fig. 4A): $B^3\Pi_1$, $c^3\Sigma^+_{\Omega=0,1}$, and $b^3\Pi_{\Omega=0,2}$. Of these, only the $c^3\Sigma^+_1$ levels have previously been observed in the near-threshold regime (*28*), and our measurement agrees to within 1 GHz. To identify the vibrational progressions, we fit the LeRoy-Bernstein (LB) dispersion model (*29*) to our observed resonances. Near threshold, the vibrational quantum number v' ($v' = -1$ is the highest bound state) is related to the binding energy by

$$E_{v'} = -\frac{1}{C_6^{1/2}}\left[2\hbar\left(\frac{2\pi}{\mu}\right)^{1/2}\frac{\Gamma(7/6)}{\Gamma(2/3)}(v' - v'_0)\right]^3 \quad (1)$$

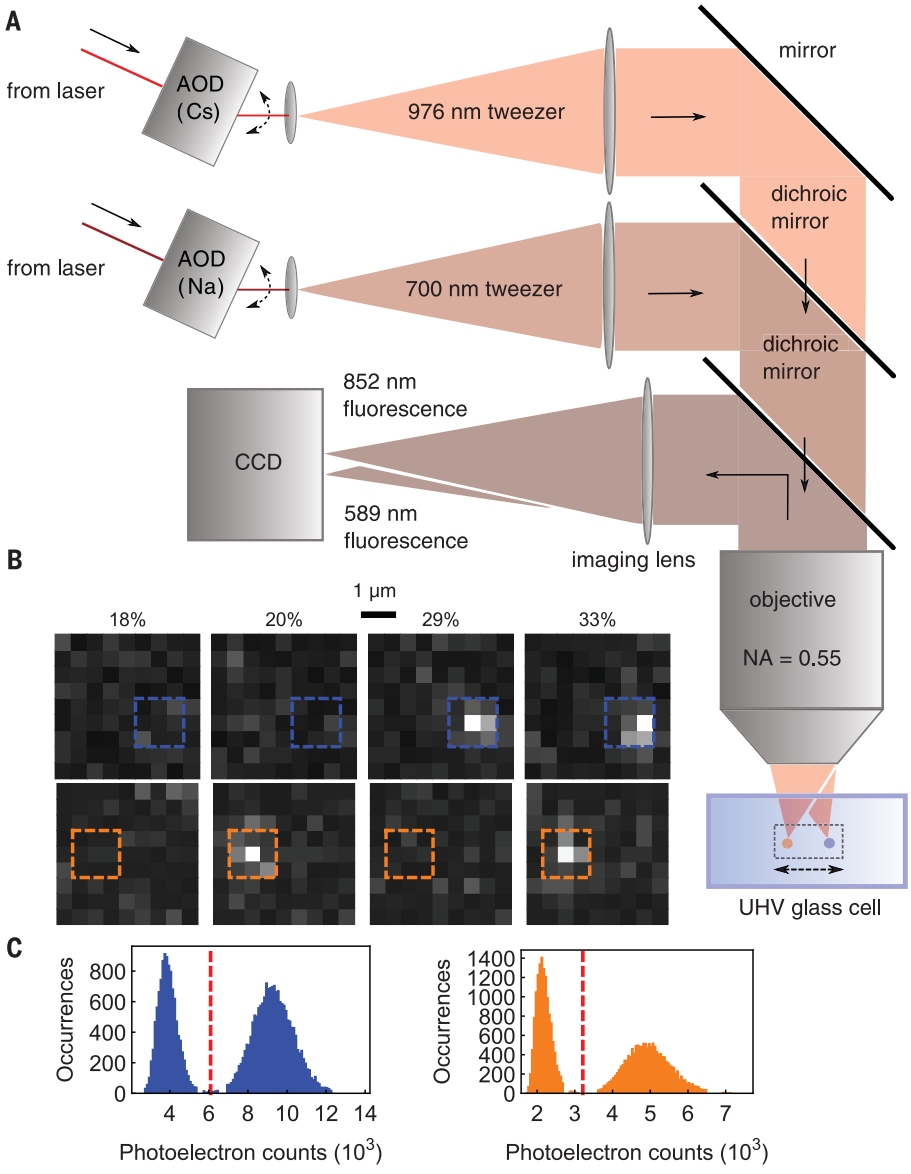

Fig. 1. Dual-species single-atom trapping and imaging. (**A**) Schematic of the setup. Optical tweezer atom-trapping beams (700 and 976 nm wavelengths) are independently steered by AODs, expanded by telescopes, and then combined on a dichroic mirror before being focused by the objective into a glass cell. Fluorescence from trapped Na and Cs atoms is collected through the objective onto the charge-coupled device camera. (**B**) Fluorescence images of single Na and Cs atoms. Length scale of 1 μm is indicated. Cs (top) and Na (bottom) are imaged sequentially in the same field of view. The four possible cases are shown with their initial loading probabilities: no atoms, a single Na atom, a single Cs atom, or both Na and Cs atoms. Dashed blue (Cs) and orange (Na) boxes indicate the regions of interest for determining the presence of atoms. (**C**) Histogram of Cs (blue) and Na (orange) fluorescence. The bimodal distribution shows clear separation between zero- and one-atom peaks. Red dashed lines indicate the threshold that is used to determine the presence of an atom.

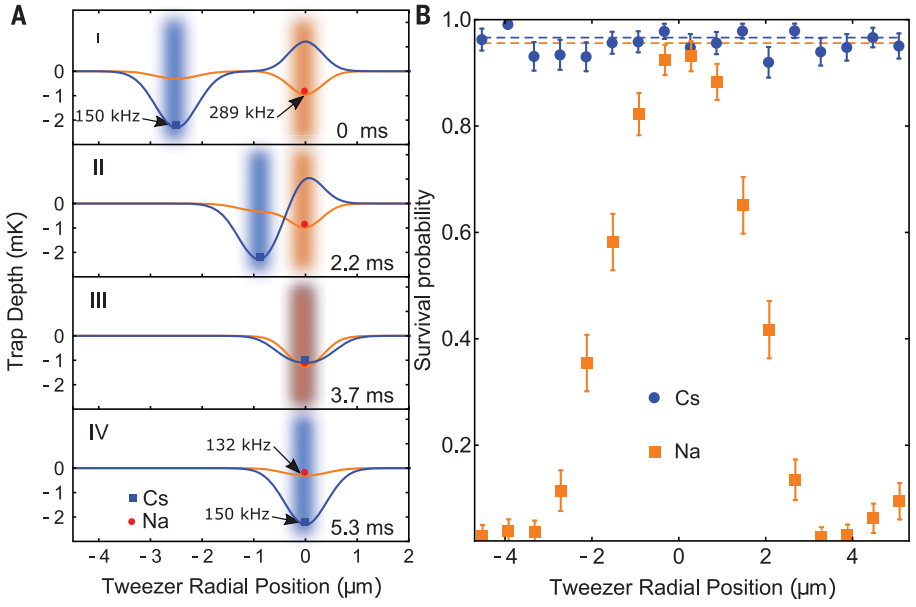

Fig. 2. Merging single Na and Cs atoms, which are initially separated by 3 μm, into one tweezer. (**A**) One-dimensional cuts of the combined, time-varying 700- and 976-nm tweezer potentials for both atoms during the merge sequence. Na and Cs are represented by dots that track the minima of their potentials (orange, Na; blue, Cs). Overlaid are graphics of the optical tweezers. Radial trap frequencies are labeled in the first and last panels (axial trap frequencies are roughly 6 times smaller). I to III depict the merging process. In IV, the 700-nm tweezer has been extinguished, and only the 976-nm tweezer remains. (**B**) Measured survival probability of Na and Cs after the sequence depicted in (A), followed by separating the tweezers through a reverse sequence to image the atoms. The two atoms are merged into the same tweezer at the survival maximum for Na. Error bars denote the Wilson score interval. The dashed lines represent the survival rates due to imperfect reimaging.

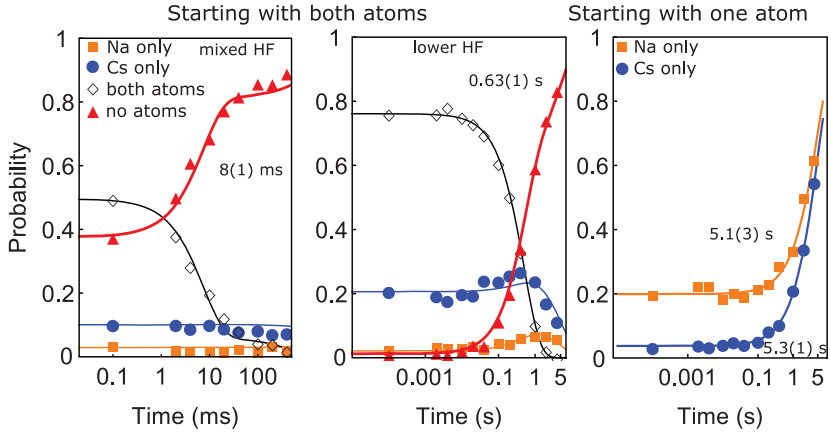

Fig. 3. Collisions of Na and Cs. The hold time in the merged trap is varied so as to measure the evolution of trap occupancy owing to various collision mechanisms. Post-selection on initial and final trap occupancies allows us to distinguish one- and two-body processes. The fastest time scales are indicated next to the thick fitted curves. The fits are explained in the supplementary materials. (**Left**) For both atoms in a mixture of hyperfine states, the loss is dominated by rapid two-body hyperfine-state-changing collision-induced loss. (**Middle**) For both atoms in their lowest hyperfine states, the loss is explained by two-body hyperfine-state-changing collisions that follow off-resonant scattering of trap light. In both the left and middle, different markers denote the final trap occupancy. (**Right**) One-body loss gives background gas limited lifetime of ~5 s for both atoms. We post-select on empty final tweezers, and markers denote initial trap occupancy.

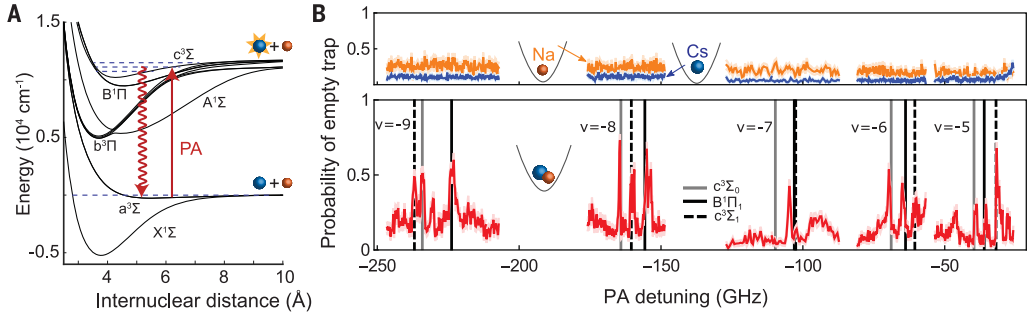

Fig. 4. PA spectroscopy of NaCs*. (**A**) NaCs molecular potentials as a function of internuclear distance (*27*). PA light excites the ground-state atoms to vibrational levels of the NaCs* excited molecular potentials, from which they mostly decay to vibrationally excited electronic ground-state molecules (red wavy line). The long-range asymptotes of the excited state potentials (dominated by van der Waals interactions in the heteronuclear molecules) correspond to one of two cases: ground-state Na colliding with excited Cs in either the lower-energy $6P_{1/2}$ (D1 line) or higher-energy $6P_{3/2}$ state (D2 line). (**B**) The probability of single Na (orange), single Cs (blue), and joint Na^+Cs (red) atoms evolving to the "no atoms" detection channel as the PA light is detuned from the Cs D2 line dissociation threshold at 351,730 GHz. When both atoms are initially loaded into the tweezer (bottom), two-body loss resonances appear because of molecule formation. As a validation of our method, we checked that no loss resonances were observed when only one atom was present (top). The positions of the loss resonances are fitted with the LB dispersion model in Eq. 1 in order to identify three different potentials and fit the respective C_6 dispersion coefficients. The expected resonance positions based on these fits are marked by vertical lines, as indicated in the legend. Except for $v = -7$, the root mean square deviation of the fitted dispersion curve from the measured frequencies are 0.3, 0.6, and 0.8 GHz for the $c^3\Sigma_1$, $c^3\Sigma_0$, and $B^1\Pi_1$ states, respectively. At $v = -7$, a crossing of molecular energy levels causes the measured spectrum to deviate from the prediction according to Eq. 1. Unassigned lines in the spectrum are likely due to rotational and hyperfine structure and predissociating potentials.

where μ is the reduced mass, and $\hbar$ is the reduced Planck's constant. We extracted the C_6 dispersion coefficients that characterize the $1/r^6$ component of the potentials and v'_0, which is an offset between –1 and 0.

Fitting to the positions of our observed $c^3\Sigma_1^+$ resonances gives $v_0 = -0.79$ and $C_6 = 8.5(6) \times 10^3$ au (atomic units), which is in agreement with the theoretical value $C_6 = 7.96 \times 10^3$ au (*30*). From the remaining loss resonances, we identified two additional progressions ($B^1\Pi_1$ and $c^3\Sigma_0^+$) with $C_6 = 1.42(33) \times 10^4$ au and $C_6 = 1.47(26) \times 10^4$ au (Fig. 4B). Both values are near the theoretical value of $C_6 = 1.83 \times 10^4$ au (*30*). Our state labels correspond to the molecular wave functions in the near-threshold regime and differ from the labels in (*30*) because of an avoided crossing, as noted in (*31*). Here, the assignment of the $c^3\Sigma_1^+$ progression is based on previous observation of the same resonances (*28*), whereas $B^1\Pi_1$ continues a previously observed sequence (*31*). The remaining progression corresponds to $c^3\Sigma_0^+$ because this is the only other compatible state. We interpret the PA spectrum as clear evidence for molecule formation because the resonance peaks appear exclusively as simultaneous loss of Na and Cs, and the resonance frequencies agree with independent measurements.

Our technique can in principle be extended beyond the simple bialkalis demonstrated here and to produce deeply bound molecules. Molecules in a single-quantum state could be created through coherent transfer (*32*, *33*) of atoms prepared in the motional ground state (*34*–*37*). Dipolar molecules trapped in a configurable array of optical tweezers (*38*, *39*) would constitute a new type of qubit for quantum information processing (*40*) and an important resource with which to explore quantum phases (*41*, *42*).

REFERENCES AND NOTES

1. D. R. Herschbach, *Angew. Chem. Int. Ed. Engl.* **26**, 1221–1243 (1987).
2. Y. T. Lee, *Angew. Chem. Int. Ed. Engl.* **26**, 939–951 (1987).
3. A. B. Henson, S. Gersten, Y. Shagam, J. Narevicius, E. Narevicius, *Science* **338**, 234–238 (2012).
4. W. E. Perreault, N. Mukherjee, R. N. Zare, *Science* **358**, 356–359 (2017).
5. S. Ospelkaus *et al*., *Science* **327**, 853–857 (2010).
6. K.-K. Ni *et al*., *Nature* **464**, 1324–1328 (2010).
7. M. H. G. de Miranda *et al*., *Nat. Phys.* **7**, 502–507 (2011).
8. K. Liu, *Annu. Rev. Phys. Chem.* **52**, 139–164 (2001).
9. X. Yang, *Annu. Rev. Phys. Chem.* **58**, 433–459 (2007).
10. A. Klein *et al*., *Nat. Phys.* **13**, 35–38 (2016).
11. L. Ratschbacher, C. Zipkes, C. Sias, M. Köhl, *Nat. Phys.* **8**, 649–652 (2012).
12. S. A. Moses *et al*., *Science* **350**, 659–662 (2015).
13. P. Puri *et al*., *Science* **357**, 1370–1375 (2017).
14. D. M. Eigler, E. K. Schweizer, *Nature* **344**, 524–526 (1990).
15. P. J. Dagdigian, L. Wharton, *J. Chem. Phys.* **57**, 1487–1496 (1972).
16. N. Schlosser, G. Reymond, I. Protsenko, P. Grangier, *Nature* **411**, 1024–1027 (2001).
17. M. S. Safronova, B. Arora, C. W. Clark, *Phys. Rev. A* **73**, 022505 (2006).
18. A. Fuhrmanek, R. Bourgain, Y. R. P. Sortais, A. Browaeys, *Phys. Rev. A* **85**, 062708 (2012).
19. P. Sompet, A. V. Carpentier, Y. H. Fung, M. McGovern, M. F. Andersen, *Phys. Rev. A* **88**, 051401 (2013).
20. N. R. Hutzler, L. R. Liu, Y. Yu, K.-K. Ni, *New J. Phys.* **19**, 023007 (2017).
21. J. Beugnon *et al*., *Nat. Phys.* **3**, 696–699 (2007).
22. A. M. Kaufman *et al*., *Science* **345**, 306–309 (2014).
23. B. Ueberholz, S. Kuhr, D. Frese, D. Meschede, V. Gomer, *J. Phys. At. Mol. Opt. Phys.* **33**, L135–L142 (2000).
24. Materials and methods are available as supplementary materials.
25. R. A. Cline, J. D. Miller, M. R. Matthews, D. J. Heinzen, *Opt. Lett.* **19**, 207 (1994).
26. K. M. Jones, E. Tiesinga, P. D. Lett, P. S. Julienne, *Rev. Mod. Phys.* **78**, 483–535 (2006).
27. M. Korek, S. Bleik, A. R. Allouche, *J. Chem. Phys.* **126**, 124313 (2007).
28. A. Grochola *et al*., *Phys. Rev. A* **84**, 012507 (2011).
29. R. J. LeRoy, R. B. Bernstein, *J. Chem. Phys.* **52**, 3869–3879 (1970).
30. M. Marinescu, H. Sadeghpour, *Phys. Rev. A* **59**, 390–404 (1999).
31. A. Grochola, P. Kowalczyk, W. Jastrzebski, *Chem. Phys. Lett.* **497**, 22–25 (2010).
32. K. Bergmann, H. Theuer, B. W. Shore, *Rev. Mod. Phys.* **70**, 1003–1025 (1998).
33. L. R. Liu *et al*., arXiv:1701.03121 [physics.atom-ph] (2017).
34. C. Monroe *et al*., *Phys. Rev. Lett.* **75**, 4011–4014 (1995).
35. X. Li, T. A. Corcovilos, Y. Wang, D. S. Weiss, *Phys. Rev. Lett.* **108**, 103001 (2012).
36. A. M. Kaufman, B. J. Lester, C. A. Regal, *Phys. Rev. X* **2**, 041014 (2012).
37. Y. Yu *et al*., arXiv:1708.03296 [physics.atom-ph] (2017).
38. D. Barredo, S. de Léséleuc, V. Lienhard, T. Lahaye, A. Browaeys, *Science* **354**, 1021–1023 (2016).
39. M. Endres *et al*., *Science* **354**, 1024–1027 (2016).
40. D. DeMille, *Phys. Rev. Lett.* **88**, 067901 (2002).
41. N. Y. Yao, M. P. Zaletel, D. M. Stamper-Kurn, A. Vishwanath, *Nat. Phys.* **14**, 405–410 (2018).
42. B. Sundar, B. Gadway, K. R. Hazzard, *Sci. Rep.* **8**, 3422 (2018).

ACKNOWLEDGMENTS

We thank R. González-Férez, P. Julienne, D. DeMille, and C. Regal for discussions. K.-K.N. thanks D. S. Jin for encouragement to pursue the research presented here. **Funding:** This work is supported by the Arnold and Mabel Beckman Foundation as well as the AFOSR Young Investigator Program, the NSF through the Harvard-MIT CUA, and the Alfred P. Sloan Foundation. **Author contributions:** L.R.L., J.D.H., Y.Y., J.T.Z., N.R.H., T.R., and K.-K.N. performed the experiment. L.R.L., J.D.H., T.R., and K.-K.N. analyzed the data and wrote the manuscript. **Competing interests:** None declared. **Data and materials availability:** All data are supplied in the main paper and the supplementary materials.

SUPPLEMENTARY MATERIALS

www.sciencemag.org/content/360/6391/900/suppl/DC1
Materials and Methods
Supplementary Text
Fig. S1
Table S1
Reference (*43*)

15 January 2018; accepted 3 April 2018
Published online 12 April 2018
10.1126/science.aar7797

Building one molecule from a reservoir of two atoms

L. R. Liu, J. D. Hood, Y. Yu, J. T. Zhang, N. R. Hutzler, T. Rosenband and K.-K. Ni

Science **360** (6391), 900-903.
DOI: 10.1126/science.aar7797originally published online April 12, 2018

Lighting the way to molecules, one by one

When chemists run reactions, what they are really doing is mixing up an enormous number of reacting partners and then hoping that they collide productively. It is possible to manipulate atoms more deliberately with a scanning tunneling microscope tip, but the process is then confined to a surface. Liu *et al.* directly manipulated individual atoms with light to form single molecules in isolation (see the Perspective by Narevicius). They used optical tweezers of two different colors to selectively steer ultracold sodium (Na) and cesium (Cs) atoms together. A subsequent optical excitation formed NaCs.

Science, this issue p. 900; see also p. 855